Frequency Models and Control in Normal Operation: the Sardinia Case Study

Frequency Models and Control in Normal Operation: the Sardinia Case Study

Francesco Arrigo
Dipartimento Energia "Galileo Ferraris"
Politecnico di Torino
Torino, Italy
francesco.arrigo@polito.it

Carmelo Mosca
Dipartimento Energia "Galileo Ferraris"
Politecnico di Torino
Torino, Italy
carmelo.mosca@polito.it

Ettore Bompard
Dipartimento Energia "Galileo Ferraris"
Politecnico di Torino
Torino, Italy
ettore.bompard@polito.it

Paolo Cuccia
Despatching Department
Terna Rete Italia S.p.A.
Torino-Cagliari, Italy
paolo.cuccia@terna.it

***Abstract*— Frequency signal is an indicator of the unbalance between the power generation and the load demand. Frequency power reserves in different timeframes are commonly deployed to keep this signal inside strict ranges around the nominal value. Reserves must be carefully dimensioned, and their dynamic performance correctly evaluated to enhance system security. This paper proposes a novel methodology to reproduce frequency fluctuations of entire days and to compute the power reserves activation dynamics by using a two-step process. Firstly, given a real power system frequency signal, a reverse aggregate model provides the unbalance in the system. Secondly, this unbalance is used to recreate and validate the original frequency signal by a forward aggregate model. After this procedure, Battery Energy Storage Systems (BESSs) are added and their impact on the frequency signal is quantified, in terms of different control schemes. The proposed method is tested in the real case of the Sardinian power system. Results show that this methodology can provide accurate estimation of the unbalance, frequency and reserves in the system, giving an understanding of the BESS impact on the frequency control.**

Keywords—battery energy storage systems, frequency control, frequency stability, normal operations, power system inertia.

I. INTRODUCTION

The environmental concerns due to the global warming are leading the power sector to deep changes in recent years, from a system based largely on fossil fuels to one based on non-dispatchable renewable energy sources (NDRES) [1]. NDRES technologies as solar and wind power plants are variable in their output ranging from almost zero to nearly full installed capacity depending on the weather conditions. Moreover, these plants are interconnected to the grid through power electronic devices, which decouple the generator from the system, providing no inertia, impacting the system stability and strength due to the limited overloading capabilities [2]. Transmission System Operators (TSOs) make use of conventional generation to regulate the system frequency and ensure frequency stability. As these power plants are being pushed out of the market, power systems may be subject to higher rate of change of frequency (ROCOF) and more extreme frequency oscillations following a system disturbance. In the future, it is expected that NDRESs will be able to provide frequency support to the grid, emulating the behaviour of synchronous generators [3] or using grid-forming technologies [4]. To provide such reserves, the NDRESs should keep some head to their maximum production. This leads to a waste of primary energy source and does not guarantee that they can provide a reliable frequency control due to the primary resource's variability. In the case of wind turbines, frequency control is also possible by making use of the kinetic energy stored in the turbine blades [5], but the amount of energy that can be released is limited and needs to be restored immediately after the transient endangering the grid stability.

In this context battery energy storage systems (BESSs) represent a promising solution to maintain power system stability and to provide ancillary services. National Grid in UK developed the "enhanced frequency response" service to address the issue of the reduced inertia [6]. At the same time, BESSs are used in the Australian [7] and Central Europe [8] frequency control market where they were able to successfully deliver a fast control and at the same time lower the TSOs costs related to the reserve provision. In literature, a large group of studies focus on the impact of BESSs after a contingency: a variety of probabilistic approaches and optimization techniques can be used to precisely quantify and improve the BESS performance [9][10]. Another group concentrates on multiple hours/day simulations. In this case, the main difficulty is to reproduce a realistic frequency oscillation which is essential to measure the BESSs potential. In general, frequency dynamics are formed by stochastic frequency deviations due to load and renewables fast power changes and deterministic frequency deviations caused by the long term mismatch between synchronous generators and the net load due to the market structure [11]. In work like [12][13] real data of wind power swings or stochastic noises such as the Ornstein-Uhlenbeck are used without considering the presence of deterministic frequency deviations. In [14], the impact of a BESS is evaluated considering different storage capacities and variable droop strategies. To reproduce the frequency, a procedure based on the Fourier transform is used where frequency oscillations have similar harmonic content with respect to real data inside a 6-hour window. Simulated frequency is different from real data, but it has the same dynamic behaviour inside this time window. In [15] a procedure to reproduce real data frequency signal is implemented but the frequency reserves intervention cannot be precisely simulated, making difficult to assess the performance of new resources.

As today, ENTSO-E presents principles for evaluating large-scale energy storage projects in terms of Cost-Benefit Analysis (CBA) in a similar way as transmission projects [16].

However, the CBA methodology does not seem able to capture the ancillary and flexibility benefits of the storage. According to ACER, more information is needed on the modelling and simulation of storage projects; in this sense it is fundamental how to quantify the real benefits of BESSs to the grid when performing frequency control during the day [17].

This paper proposes a method to reproduce frequency fluctuations by using a two-step process: a reverse aggregate model provides the unbalance in the system which is used to recreate the original frequency signal by a forward aggregate model. The models consider the European Load Frequency Control (LFC) schemes and allow the analysis of contingencies and normal operation, with evaluation and quantification of the BESS impact on the frequency dynamics. The models are tested and validated using the real data of the insular power system of Sardinia in Italy.

The outline of this paper is as follows: Section II gives a brief overview of the frequency regulation schemes adopted in Europe and in this study. Section III describes the implemented models to reproduce the real frequency signal and provides an example of a simulated contingency. In Section IV the methodology is applied in a normal day of frequency oscillations of the Sardinian system, which is used as a base scenario to quantify the BESS contribution in stabilizing frequency. Section VI concludes the paper.

II. Frequency Regulation in Power Systems

In the Continental Europe (CE) synchronous zone, the power-demand variations are addressed by the LFC scheme, which comprises in a temporal sequence the Frequency Containment Process (FCP, primary), automatically activated to stabilize the frequency deviation using the Frequency Containment Reserve (FCR, secondary), the Frequency Restoration Process (FRP), automatically and manually activated in the area where the imbalance occurs to return frequency to its nominal value using the Frequency Restoration Reserve (FRR), and the Replacement Reserve Process (RRP, tertiary) manually activated to replace the activated FRR using the Replacement Reserve (RR). Control actions are performed in different successive steps, each with different characteristic and qualities, and all depending on each other [19], as showed in Fig. 1. For example in Italy, FCR is a mandatory service for all generating units (except the non-programmable ones) with a power higher than 10 MW and it was decided recently to remunerate it [20]. FRR and RR are remunerated in the Dispatching Service Market (MSD).

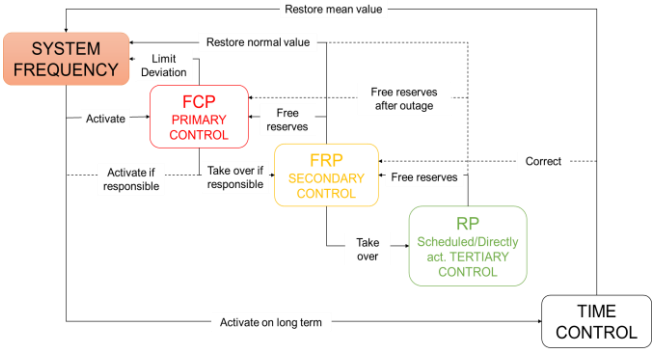

Fig. 1. Load frequency control scheme and actions starting with the system frequency, elaborated from [19].

FCP allows to re-establish the system frequency in response to a sudden power-demand imbalance. It is a local regulation of the generator's speed. The regulating energy of a unit is the ratio between the active power variation and the frequency variation that caused the regulator intervention. For the FCP, units must provide half of the FCR in a maximum delay of 15 s and the entire reserve within 30 s after the perturbation. They must continue to deliver power at least for 15 minutes. The units that participate to the FCP must guarantee an active power reserve greater than ±1,5% of the efficient power for the continent and ±10% for Sardinia and Sicily (in insulated condition). The dead band must be not higher than ±10 mHz. The droop σ_p of a unit is the ratio between the frequency variation Δf (in pu of nominal frequency f_0 and the corresponding active power variation ΔP_e, measured in steady state and in pu of the efficient power of the group.

$$\sigma_p = -\frac{\Delta f / f_n}{\Delta P_e / P_{eff}} \times 100 \quad (1)$$

The regulating energy is correlated to the droop:

$$E_p = -\frac{P_n}{f_0 \sigma_p} \quad (2)$$

The function of FRP is to restore the system frequency to its set point value and the areas interchanges to their scheduled values. The FRP is made by the same power regulators that intervene in the FCP, but using a signal, the Regulating Level, sent by the Grid Regulator, an automatic centralized device. The Grid Regulator is sensible to the Area Control Error (ACE), calculated using the frequency deviation and the exchanged power error ΔP_S between the control areas:

$$\varepsilon_r = k_{rs} \Delta f + \Delta P_S \quad (3)$$

where k_{rs} is the participation factor of the control area. The Grid Regulator is a proportional-integral controller and it calculates the regulating level to be send to the units that participate to the FRP:

$$l = -\frac{100}{P_D}\left(\beta \varepsilon_r + \frac{1}{T}\int \varepsilon_r dt\right) + 50 \quad (4)$$

where β and T are parameters imposed by the TSO and P_D is the total FRR. The level is a value between 0 (corresponding to the minimum of the FRR band) and 100 (corresponding to the maximum of the FRR band). A value $l = 50$ means the unit to keep its scheduled value for generation. The units participating to the FRP must guarantee an active power reserve greater than ±6% of the efficient power for thermal units and ±15% for hydro units.

Finally, in Art. 131 of [18], seven frequency quality criteria are reported to evaluate frequency stability. In this paper, we simply compute the mean value f_m and the standard deviation σ of the frequency.

III. Adopted Models for Frequency Dynamics Studies

A. The Forward and Reverse Aggregate Models

The dynamic behaviour of a synchronous generating unit in a power system is determined by the swing equation. After a disturbance, like a loss of generation, the speed of the machines in different parts of a large power system varies with different trajectories. However, synchronism is retained among the machines and the frequency stability is determined by the overall system response as described by the Centre-of-Inertia frequency [23]. This mean frequency can be evaluated by making use of an aggregated dynamic model, which can estimate the essential characteristics of a synchronously

isolated system's frequency response considering not all the generator dynamics and characteristics, but the mean frequency fluctuations [24]. Considering the inertia constant of the single generating units, the aggregated inertia of the system is:

$$H_{sys} = \frac{\sum_{i=1}^{N} S_{ni} H_i}{\sum_{i=1}^{N} S_{ni}} = \frac{E_{k,sys}}{S_{tot}} \quad (7)$$

where S_{ni} is the rated power of generator i [MVA], H_i is the inertia constant of generator i [s], $E_{k,sys}$ is the system rotational energy [MWs] and S_{tot} is the total rated power of the generators [MVA]. It is possible to derive then the aggregated swing equation for the whole system, given a generation-load imbalance ΔP_L:

$$\frac{df}{dt} = \frac{f_0}{2H_{sys}S_{tot}} (\Delta P_m - \Delta P_L + D \cdot \Delta f) \quad (8)$$

where ΔP_m is the power produced by the regulating resources in the grid; ΔP_L includes the eventual presence of a contingency, for example the trip of a generator and/or the power fluctuations caused by stochastic ΔP_{sto} and deterministic ΔP_{det} frequency deviations due to the unit commitment scheduling; D represents the load damping coefficient due to the load frequency dependency.
The terms in equation (8) can be written as:

$$\Delta P_m = \Delta P_{PRI} + \Delta P_{SEC} + \Delta P_{TER} \quad (9)$$

$$\Delta P_L = \Delta P_{sto} + \Delta P_{det} + \Delta P_{cont} \quad (10)$$

where ΔP_{PRI} is the FCP contribution, ΔP_{SEC} is the FRP contribution and ΔP_{TER} is the RP contribution.

When using the generation-load imbalance ΔP_L as input, we can derive the frequency behavior using the aggregate model in a "forward" mode. The Forward model can be seen in Fig. 2 and it is formed by: 1) System inertia and load damping block; 2) Resources power plant transfer functions which model a unique equivalent power plant model for each typology (hydro, steam, gas etc…) present in the grid; 3) FCP, FRP and RRP control models.

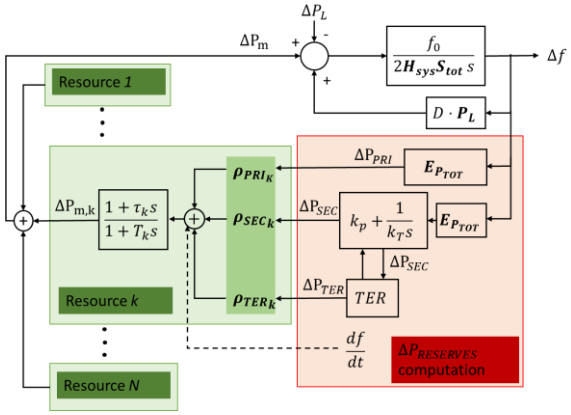

Fig. 2. Main components of the forward model.

The block parameters are:

- The equivalent power plant zero-time constant τ [s] and pole-time constant T [s]. For steam generator two additional poles are used to model its dynamics [23].
- The system inertia $\frac{f_0}{2H_{sys}S_{tot}}$ $[\frac{MWs}{Hz}]$ and the constant load regulating energy $E_c = D_L P_L$ $[\frac{MW}{Hz}]$, where D_L is the change of load under percentage in frequency and P_L is the total load of the system changing during the day.
- The permanent regulating energy $E_{P_{TOT}} = \sum_k \frac{P_{n_k}}{f_0 d}$ [MW/Hz], where d is the power plant droop and P_{n_k} is the machine nominal active power.
- The proportional k_p and integral k_T constant of the FRP regulation (ΔP_s term from Eq. (3) is dropped for synchronous isolated areas).
- The machine participation factors $\rho_{PRI_k} = \frac{E_{P_k}}{E_{P_{TOT}}}$, $\rho_{SEC_k} = \frac{P_{n_k}}{P_{n_{TOT}}}$ and ρ_{TER_k} for FCP, FRP and RRP respectively are applied to each resource participating to frequency control.
- Dead bands, saturations and ramp rate limiters are added to generators and controllers' blocks if needed.

Parameters in bold in Fig. 2 vary during the simulation to reflect real changes in the system at different times. RRP is implemented assuming that RR are ready, and it can be called by the TSO when requested. We assume the RR is called when the FRR reaches almost its maximum or minimum acceptable level l, which is equal respectively to TER_{up} and TER_{dw} as defined by the user. After the RR is activated, it starts as a ramp and it is stopped when the FRR is restored decreasing the regulating level. The ramp is formulated as follows:

$$\Delta P_{TER}(t) = FRR_{TOT} * \frac{t - t_0}{TER_{time} - t_0} \quad (11)$$

where $\Delta P_{TER}(t)$ is the RR requested at time t, FRR_{TOT} is the total FRR and TER_{time} is the timeframe in which the RR needs to be fully activated and t_0 is the starting activation time. The RRP is stopped when the level is $48 < l < 53$.

The aggregate model is basically a transfer function, which can be inverted obtaining the "reverse" model starting from Eq. (8-9-10). The "reverse" model can estimate the generation-load imbalance based on two inputs: the frequency signal Δf_{REAL} and its numerical derivative. All the blocks and parameters are equal to the forward model. As shown in next Section II.B, if we feed the computed load unbalance ΔP_{mis} from the reverse model in the forward model, we can reproduce the original frequency signal $\Delta f_{SIM_{real}}$. Then, it is possible to consider new resources added into the system like BESSs or modify model parameters (e.g. reduced inertia) and compute a new frequency signal $\Delta f_{SIM_{new}}$. In this way we quantify the direct impact of a BESS in the grid. Fig. 3 reports a schematic view of the proposed methodology.

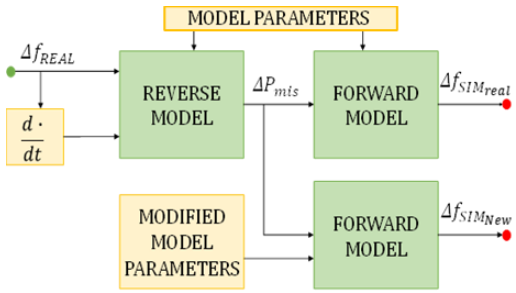

Fig. 3. Flowchart of the proposed approach to study the frequency dynamics.

B. BESS Model and Regulation

The dynamic model used for the BESS is described in [24] . An Equivalent Saturation Logic (ESL) is used to tune the control parameters of the BESS and the power band is divided between primary and inertial control. The virtual inertia contribution K_B is calculated as:

$$K_b = \frac{2H_B P_B}{f_0};\ with\ H_B = \frac{f_0 \chi_B}{2\left|\frac{df}{dt}\right|_{MAX}} \quad (12)$$

where χ_B is the share of participation in the inertial control of the total power of the BESS, whereas 1-χ_B represents the share of participation in the primary control. $\left|\frac{df}{dt}\right|_{MAX}$ is the maximum ROCOF value (in this study 1 Hz/s) a generator should sustain during contingencies, at which we assume to saturate the contribution of the BESS. The FCP contribution is calculated as:

$$E_{P_B} = \frac{P_B(1-\chi_B)}{d_B f_0} \quad (13)$$

where P_B is the nominal active power of the BESS, and $d_B$is evaluated using the ESL:

$$d_B = \frac{\Delta f_{MAX}}{f_0}\left(\frac{P_n}{\Delta P_{MAX}}\right)_B \quad (14)$$

In the case of conventional plants, as mentioned earlier, the power band for FCR is $\frac{\Delta P_{MAX}}{P_n} = 10\%$ in Sardinia, whereas the BESS use $(1-\chi_B)$ of their band. Consequently, a new equivalent value for the droop can be computed, imposing for the BESS the saturation of its reserve at the same frequency deviation of a conventional unit.

An additional share $P_{B_{SEC}}$ of P_B can be used for the FRP. The total FCR is sent to the BESS using the participation factor $\rho_{SEC_B} = \frac{P_{B_{SEC}}}{P_{SEC_{TOT}}}$, where $P_{SEC_{TOT}}$ is the total FRR.

C. Contingency Validation

A typical contingency is applied to the forward model to analyze the correct LFC activation. The ΔP_L is 250 MW and it is simulated as a ramp of 1 second; the characteristics and parameters of the system are the ones used in the next section case study. In Fig. 4 frequency and power reserves profiles after the contingency are shown, with a zoom over the first 100 s: after a first decay, the frequency is stabilized by the FCR and then returns to nominal value thanks to the FRR activation. RR activates when FRR signal level reach saturation (200 MW of FRR is used with a $TER_{up} = 85$). Using the evaluated frequency and the reverse model is then possible to reconstruct the ΔP_{mis} as shown in Fig. 5 and compare it with the original ramp: the two trajectories are equal except for very small differences around the cuspid points at 5 and 6 seconds due to small imprecisions of the numerical methods of the solvers.

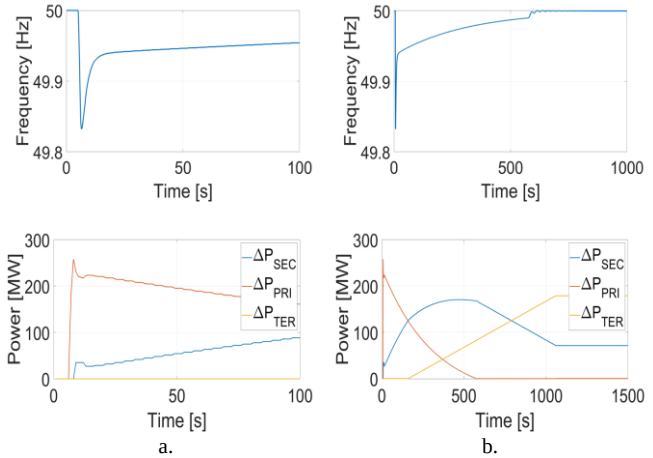

Fig. 4. Frequency and power reserve profiles during the contingency event: a. first 100 s; b. 1500 s.

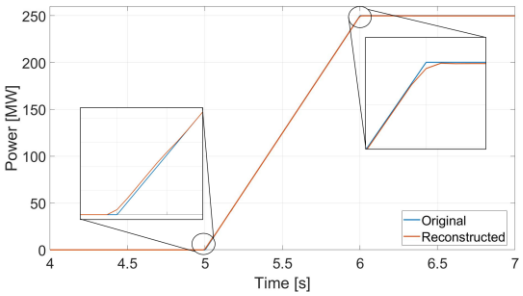

Fig. 5. Original ΔP_L and reconstructed ΔP_{mis} profiles with zooms on cuspid points.

IV. Case Study

A. Sardinian Power System

The Sardinian power system is a small power system (maximum load around 1500 MW) and asynchronous to the continental grid, as it is connected through two HVDC systems which provide FCR.

In a single area system, as Sardinia, there is no tie-line power mismatch ΔP_s (see Eq. (3)) to be controlled, and the FRP restores only the nominal system frequency. Table I contains the parameters to set the dynamic model of thermal, hydro and HVDC units and the parameters for FRP (proportional and integral gains) and RRP, set using values found in literature. For HVDC no dead band is considered, as dead band is imposed to traditional units for mechanical reasons which are not needed by power electronics devices without rotating masses.

TABLE I. Dynamic Data for FCR, FRR and RRP

FCR		**Zero-time constant τ [s]**	**Pole time constant T [s]**	**Droop d [%]**
	Thermal	3	10	5%
	Hydro	-1	6	4%
	HVDC	3.3	10	5%
FRP	k_p		k_T	
	0.05		300	
RRP	TER_{up}	TER_{dw}	TER_{time}	
	85	15	10 min	

B. Base Scenarios Setup and Proposed Simulations

The frequency and demand power data used for verification were obtained from the Italian TSO. The time step of the data is 15 minutes for generation and demand, and 1 second for frequency data. A base case scenario without BESSs is constructed to reproduce a whole day of frequency signal. The signal was recorded on the Sardinian grid on the 18th January 2018 (winter peak) with average equal to 50.0021 and standard deviation equal to 0.0067. The actual dispatch of regulating generators is used and therefore inertia and frequency reserves quantities vary during the day (see Fig. 6). Sardinian system had a kinetic energy with a mean value of 9.6 GWs, ranging from a minimum of 9.3 GWs to a maximum of 10.3 GWs. The number of online synchronous units was changing from 18 to 22. Two reconstructions are proposed: 1) simulation with only FCP; 2) simulation with FCP, FRP and RP, to test the proposed model capabilities. In Fig. 7 the resulting ΔP_{mis} computed by the reverse model in the first case is shown together with the frequency signal. The power mismatch between generation and consumption is specular to the frequency signal as only the FCP is present in the grid to oppose oscillations.

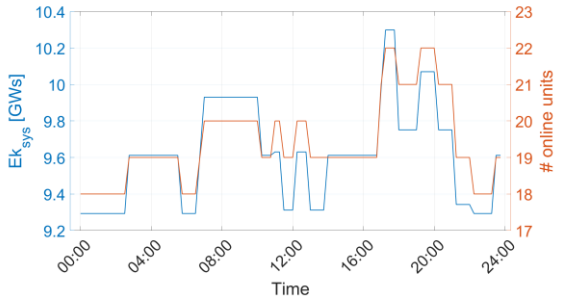

Fig. 6. Kinetic energy and number of online synchronous units in Sardinia on the 18th January 2018.

The ΔP_{mis} is used to feed the forward model and to calculate the frequency signal. The standard deviation of the error between the simulated and the real frequency is $2.03 \cdot 10^{-4}$ Hz which is negligible being much smaller than the typical dead band value of the controller (0.01 Hz). This error is mainly due to the non-linearity present in the models such as dead bands and saturations and it can also be further reduced by decreasing the maximum allowed time step of the simulations.

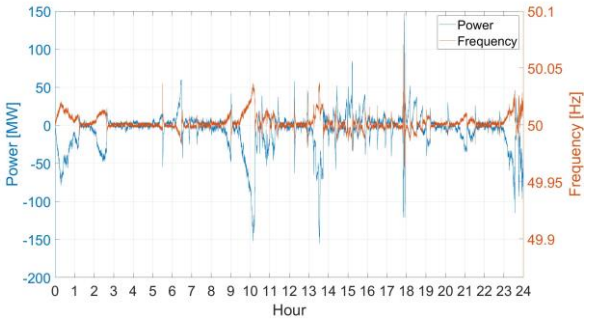

Fig. 7. Comparison between the frequency signal and the reconstructed power imbalance with only FCP.

In the second setup we show the results obtained if we consider the presence of FRP and RP schemes as CE with the Sardinia frequency signal, by simulating an FRR of 120 MW. This is only an example to show the model capabilities, but it does not represent the reality of Sardinian frequency control, which presents different FRR and RR from the CE ones. The frequency error is similar in magnitude to the previous case with a standard deviation slightly higher than before, equal to $2.4 \cdot 10^{-4}$ Hz. In Fig. 8 the three frequency reserves profiles (FCR, FRR and RR) are shown. The ΔP_{TER} is continuously decreasing during the day since the frequency of the examined day is on average around 50.0021 Hz, higher than 50 Hz, and the FRR is therefore continuously decreasing. We can estimate analytically the sum of FRR and RR activated by integrating the ACE during the day:

$$k_P \cdot \Delta f + \int_o^{24h} \frac{E_{P_{TOT}} \cdot \Delta f}{k_T} \cong \frac{\overline{E_{P_{TOT}}} \cdot \overline{\Delta f}}{k_T} \cdot 24h = 2736\, MW$$

where $\overline{\Delta E_{P_{TOT}}}$ and $\overline{\Delta f}$ are the mean values during the day. The result is very close to the simulated sum of FRR and RR, as we can see in Fig. 8, at the final timestep. It is possible to see the FCR, which follows the generation-demand mismatch due to the HVDC without dead band in the FCP, while the RR is called during the day to restore the FRR. The FRR is activated to bring the frequency value to the nominal value.

C. BESS results

The first setup proposed in previous section has been considered as reference case to test the BESS addition. The technical impact of a BESS in fixed droop and with FC and FR control operation mode is evaluated.

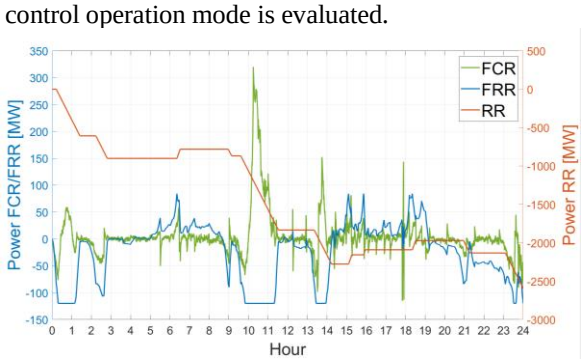

Fig. 8. FCR, FRR and RR simulated profiles based on the frequency signal of the 18th January 2018.

The FCP of the BESS is divided in inertial and primary response. The performance of frequency control is assessed using the indicators given in Section II.

1) Frequency Containment Process (FCP)

A sensitivity analysis is performed on the capacity, droop and the share of inertial and primary response provided by the BESS. Two systems of 50 MW and 250 MW BESSs are analysed, with a pole time constant $T_B = 0.3\, s$. For the 250 MW case, two different droops d_B of 0.005 and 0.004 are considered. The frequency response of the BESS is compared using different shares of inertial and primary response, i.e., 50% of inertial and primary control, 100% inertial control and 100% of primary control. Fig. 9 shows the frequency trend with the addition of a BESS of 250 MW in the FCP and only primary response $\chi_B = 0$, compared with the case without BESSs.

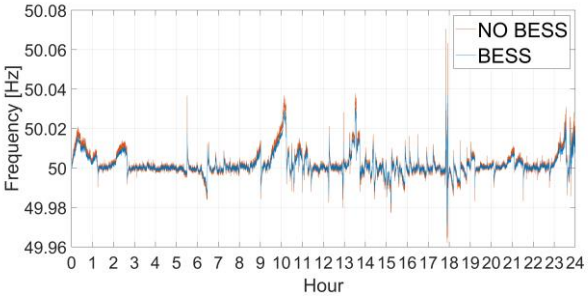

Fig. 9. Comparison between the frequency signals with and without BESSs participating in the FCP.

2) Frequency Restoration Process (FRP)

In the second case, the BESS has been used only for the FRP. The impact in the case of normal operation is higher with respect to the FCP due to the integral part in the FRP. In fact, a purely proportional action, as in the FCP, is higher when the frequency deviation is higher. The proportional action is fast and reduce the error, without compensating it. In the FRP the action is proportional to the integral of the frequency deviation and keep memory of the past deviation errors. It is higher in the case of a frequency signal unbalanced from the set-point, which is the case under examination. TABLE II. reports the results of the two cases analyzed, with participation of the BESS in the FCP and the FRP. The best performance in terms of mean frequency and standard deviation are with the participation in the FRP only, with a mean frequency reported to the nominal value from the initial 50.0021 Hz and a standard deviation improved of 45% in the case of the BESS of 50 MW (from the initial value of 0.0067 to 0.0037) and of

57% in the case of the BESS of 250 MW (from 0.0067 to 0.0029). In the case of participation in the FCP only, the best improvements can be seen in the case with the BESS of 250 MW, lower droop $d_B = 0.004$ and only primary control $\chi_B = 0$, with a mean frequency equal to 50.0016 Hz and a standard deviation improved of 24% (from 0.0067 to 0.0051).

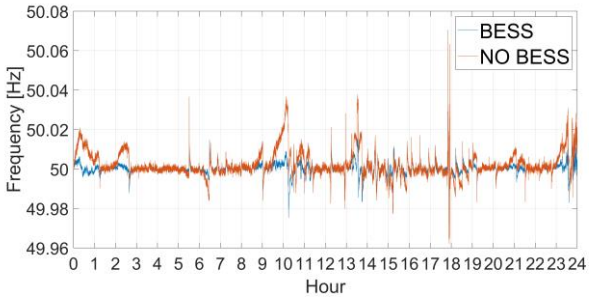

Fig. 10. Comparison between the frequency signals with and without BESSs with FR control.

TABLE II. RESULTS OF THE FREQUENCY CONTROL WITH PARTICIPATION OF THE BESS IN THE FCP AND FRP.

	f_m [Hz]	σ [Hz]	d_B	χ_B	FRP
Base	50.0021	0.0067	-	-	No
50	50.0020	0.0064	0.005	0	No
50	50.0021	0.0067	0.005	1	No
50	50.0020	0.0065	0.005	0.5	No
50	50.0000	0.0037	0.005	-	Yes
250	50.0017	0.0054	0.005	0	No
250	50.0021	0.0067	0.005	1	No
250	50.0019	0.0059	0.005	0.5	No
250	50.0018	0.0058	0.004	0.5	No
250	50.0016	0.0051	0.004	0	No
250	50.0021	0.0067	0.004	1	No
250	50.0000	0.0029	0.005	-	Yes

V. CONCLUSIONS

In this paper a methodology to reproduce frequency fluctuations and to compute the power reserves by using a two-step process has been presented and assessed. The European LFC schemes have been implemented and tested on a real case study taken from the Sardinian power system. BESS's different capabilities to support the frequency control have been analyzed and quantified. The paper shows that the impact of BESSs strictly depends on the characteristics of the services and of the frequency signal itself. In normal day oscillations, the virtual inertia control is not effective in containing the frequency oscillations, the participation of the BESS in the FCP improves lightly the frequency signal while the FRP is the most useful service. Typically frequency dynamics are characterized by cyclical slow components, therefore it is expected that slower services such as the FRP are more effective in decreasing the oscillations, while in the case of fast changes, as sudden contingencies, virtual inertia and the FCP are more important. More simulations can be performed within the proposed framework to investigate and better motivate this thesis and to understand the consequences of this services on the BESS's SoC and degradation and to quantify the benefit of BESSs to frequency control in terms of cost-benefit analysis.

ACKNOWLEDGMENT

The authors gratefully acknowledge Antonio Dimasi and Gabriele Motzo at Terna Rete Italia S.p.A. for their valuable comments and suggestions to this work.

REFERENCES

[1] European Commission. Clean Energy for all Europeans, 2019.

[2] V. N. Sewdien *et al.*, "Effects of Increasing Power Electronics on System Stability: Results from MIGRATE Questionnaire," in *2018 International Conference and Utility Exhibition on Green Energy for Sustainable Development (ICUE)*, Oct. 2018, pp. 1-9.

[3] F. Mandrile, E. Carpaneto, and R. Bojoi, "Grid-Tied Inverter with Simplified Virtual Synchronous Compensator for Grid Services and Grid Support," in *2019 IEEE Energy Conversion Congress and Exposition (ECCE)*, Sep. 2019, pp. 4317-4323.

[4] M. Ndreko, S. Rüberg, and W. Winter, "Grid forming control for stable power systems with up to 100% inverter based generation: a paradigm scenario using the IEEE 118-Bus system," in *17th Int. Wind Integration Workshop*, Oct. 2018, pp. 17-19.

[5] M. Dreidy, H. Mokhlis, and S. Mekhilef, "Inertia response and frequency control techniques for renewable energy sources: A review," *Renewable and Sustainable Energy Reviews*, vol. 69, pp. 144-155, Mar. 2017.

[6] National Grid. National Grid frequency services, 2019.

[7] Australian Energy Market Operator. Quaterly Energy Dynamics - Q1, 2019.

[8] J. Fleer and P. Stenzel, "Impact analysis of different operation strategies for battery energy storage systems providing primary control reserve," *Journal of Energy Storage*, vol. 8, pp. 320-338, Nov. 2016.

[9] P. V. Brogan, R. J. Best, D. J. Morrow, K. McKinley, and M. L. Kubik, "Effect of BESS response on frequency and RoCof during underfrequency transients," *IEEE Trans. Power Syst.*, vol. 34, no. 1, pp. 575-583, Jan. 2019.

[10] U. Markovic, V. Häberle, D. Shcetinin, G. Hug., D. Callaway, and E. Vrettos, "Optimal Sizing and Tuning of Storage Capacity for Fast Frequency Control in Low-Inertia Systems," in *2019 International Conference on Smart Energy Systems and Technologies (SEST)*, Sep. 2019, pp. 1-6.

[11] ENTSO-E, EURELECTRIC. Deterministic frequency deviations–root causes and proposals for potential solutions, 2011.

[12] J. Cao, W. Du, H. Wang, M. McCulloch, "Optimal sizing and control strategies for hybrid storage system as limited by grid frequency deviations," *IEEE Trans. Power Syst.*, vol. 33, no. 5, pp. 5486-5495, Feb. 2018.

[13] F. M. Mele, A. Ortega, R. Zarate-Minano, and F. Milano, "Impact of variability, uncertainty and frequency regulation on power system frequency distribution," in *2016 Power Systems Computation Conference (PSCC)*, Jun. 2016, pp. 1-8.

[14] F. Arrigo, E. Bompard, M. Merlo, and F. Milano, "Assessment of primary frequency control through battery energy storage systems," *Electrical Power and Energy Systems*, vol. 115, 105428, Feb. 2020.

[15] R. Lee, S. Homan, N. Mac Dowell, and S. Brown, "A closed-loop analysis of grid scale battery systems providing frequency response and reserve services in a variable inertia grid," *Applied Energy*, vol. 236, pp. 961-972, Feb. 2019.

[16] ENTSO-E. 2nd ENTSO-E Guideline for Cost-Benefit Analysis of Grid Development Projects, 2018.

[17] ACER. CBA methodologies for electricity transmission infrastructures and scenarios for energy and power system planning, 2016.

[18] European Commission. Commission Regulation (EU) 2017/1485 - Establishing a guideline on electricity transmission system operation, 2017.

[19] UCTE. Appendix 1: Load Frequency Control and Performance, 2004.

[20] TERNA. Avvio del meccanismo di remunerazione della regolazione primaria di frequenza, 2014.

[21] TERNA. Transmission system quality – Annual report, 2018. [Online].

[22] Y. Hase, T. Khandelwal, and K. Kameda, *Power System Dynamics with Computer-Based Modeling and Analysis*. New York, NY, USA: John Wiley & Sons, 2020.

[23] P. Kundur, *Power System Stability and Control*. New York, NY: McGraw-Hill, 1994.

[24] C. Mosca, F. Arrigo, A. Mazza, E. Bompard, E. Carpaneto, G. Chicco, P. Cuccia, "Mitigation of frequency stability issues in low inertia power systems using synchronous compensators and battery energy storage systems," *IET Gener., Transm. and Distrib.*, vol. 13, no. 17, pp. 3951-3959, Sept. 2019.